2930 © *1984 The Chemical Society of Japan* *Bull. Chem. Soc. Jpn., 57, 2930—2941 (1984)* [Vol. 57, No. 10

Magnetic Circular Dichroism and Electronic Absorption Spectra of Mixed (Amine)(carboxylato) Complexes with the [Pd(N)$_n$(O)$_{4-n}$]-type (n=0—4)

Kazuhiko NAKAYAMA,* Takashi KOMORITA, and Yoichi SHIMURA
Department of Chemistry, Faculty of Science, Osaka University, Toyonaka, Osaka 560

(Received March 29, 1984)

Mixed-ligand [Pd(N)$_n$(O)$_{4-n}$]-type complexes constituting a long systematic series (n=0—4) were synthesized. Ammonia, ethylenediamine, *rac*-propylenediamine, trimethylenediamine, glycinate, β-alaninate, acetate, oxalate, and malonate were employed as ligands. Their magnetic circular dichroism (MCD) and electronic absorption spectra were discussed together with the CD spectra of the corresponding optically active complexes. The results strongly suggest that the dispersion of MCD observed in the spin-allowed d-d region is primarily a composite of B terms. Moreover, the MCD in the charge transfer region was found to be qualitatively additive with respect to contributions by the constituent ligands. From a detailed examination of the spin-allowed d-d absorption bands, it is noted that the substitution of an *N,O*-ligand for an *N,N*-ligand largely affects neither the band area nor band width whereas that of an *O,O*-ligand for an *N,O*-ligand does.

The concurrent examination of absorption, magnetic circular dichroism(MCD), and CD spectra furnished useful information on the electronic structures of *cis*- and *trans*- [Pd(Cl)$_2$(N)$_2$]-type complexes.[1] In the preceding paper,[2] we reported the synthesis of a large number of mixed-ligand [Pd(N)$_n$(O)$_{4-n}$]-type complexes with at least one optically active ligand and the detailed investigation of the CD spectra.

In the present work, optically inactive [Pd(N)$_n$(O)$_{4-n}$]-type complexes were synthesized corresponding to the previous optically active comlexes,[2] and their MCD spectra were examined. Although most of the former complexes were found to be more labile than the latter, the systematized synthetic methods developed previously[2] were effective. Ammonia, ethylenediamine(en), *rac*-propylenediamine(*rac*-pn), and trimethylenediamine(tn) were employed as *N*- or *N,N*-ligands; glycinate(gly) and β-alaninate(β-ala) were as *N,O*-ligands; and acetate, oxalate(ox), and malonate(mal) were as *O*- or *O,O*-ligands. Di-μ-hydroxodipalladium complexes were also obtained. Although these complexes, if approximated by a D$_{4h}$ symmetry, are expected to exhibit A-term MCD based on $^1E_g \leftarrow {}^1A_{1g}$ in the d-d transition region, our spectral examination indicates that the contribution of the A term is minor and that inherent B terms generally predominate irrespective of the symmetries of the complexes, unlike in the case of [MCl$_4$]$^{2-}$ (M=Pt and Pd)[3] and *cis*-[Pd(Cl)$_2$(N)$_2$]-type complexes.[1] Although three or four spin-allowed d-d transitions should occur in a D$_{4h}$ or lower symmetries, the spin-allowed d-d absorption bands of the series of complexes appear only as a single broad unsymmetrical band. These bands are analyzed in terms of band area and the band shape parameters,[1] and the influence of ligands on the band shape and band area is discussed.

Experimental

[Pd(N)$_4$]-type Complexes. *1) [Pd(NH$_3$)$_4$](ClO$_4$)$_2$*: This complex was obtained by metathesis of the corresponding chloride with the calculated amount of silver perchlorate. Found: H, 3.33; N, 14.97%. Calcd for $H_{12}N_4Cl_2O_8Pd$: H, 3.24; N, 15.00%.

2) [Pd(en)(NH$_3$)$_2$]Cl$_2$: This complex was prepared in the same manner as for [Pd(*S*-pn)(NH$_3$)$_2$]Cl$_2$,[2] but ethanol was used for crystallization in place of ether. Yield: 70%. Found: C, 8.99; H, 5.20; N, 20.52%. Calcd for $C_2H_{14}N_4Cl_2Pd$: C, 8.85; H, 5.20; N, 20.64%.

3) [Pd(en)(tn)]Cl$_2$: This was prepared from [PdCl$_2$(en)] in the same way as for [Pd(*S*-pn)(tn)]Cl$_2$[2] but crystallized from a methanol–ethanol medium instead of an ethanol–ether one. Yield: 80%. Found: C, 19.23; H, 5.79; N, 17.94%. Calcd for $C_5H_{18}N_4Cl_2Pd$: C, 19.28; H, 5.82; N, 17.98%.

4) [PdL(N,N-Et$_2$en)]Cl$_2$ (L=en and tn): These complexes were prepared by methods similar to those for the corresponding (2*S*)-*N*^{1},*N*^{1}-diethyl-1,2-propanediamine(*N*^{1},*N*^{1}-Et$_2$-(*S*)-pn) complexes.[2] Yield: 75—85%. Found: C, 24.79; H, 7.20; N, 14.32%. Calcd for [Pd(en)(*N,N*-Et$_2$en)]Cl$_2$·2H$_2$O=$C_8H_{28}N_4Cl_2O_2Pd$: C, 24.66; H, 7.24; N, 14.38%. Found: C, 28.20; H, 7.31; N, 14.55%. Calcd for [Pd(tn)(*N,N*-Et$_2$en)]Cl$_2$·H$_2$O=$C_9H_{28}N_4Cl_2OPd$: C, 28.03; H, 7.32; N, 14.53%.

5) [PdL$_2$]Cl$_2$ (L=N,N-Et$_2$en and N,N,C,C-Me$_4$en):[4] These were obtained in a way similar to that for [Pd(*N*^{1},*N*^{1}-Et$_2$-(*S*)-pn)$_2$]Cl$_2$.[5] Found: C, 35.15; H, 7.92; N, 13.63%. Calcd for [Pd(*N,N*-Et$_2$en)$_2$]Cl$_2$=$C_{12}H_{32}N_4Cl_2Pd$: C, 35.18; H, 7.87; N, 13.67%. Found: C, 32.40; H, 8.14; N, 12.61%. Calcd for [Pd(*N,N,C,C*-Me$_4$en)$_2$]Cl$_2$·2H$_2$O=$C_{12}H_{36}N_4Cl_2O_2Pd$: C, 32.33; H, 8.14; N, 12.57%.

6) Other Complexes: The complexes [Pd(en)$_2$]Cl$_2$ and [Pd(tn)$_2$]Cl$_2$ were obtained according to the method described in the literature[6] or the one similar to it. Found: C, 16.18; H, 5.43; N, 18.83%. Calcd for [Pd(en)$_2$]Cl$_2$=$C_4H_{16}N_4Cl_2Pd$: C, 16.15; H, 5.42; N, 18.83%. Found: C, 22.20; H, 6.24; N, 17.14%. Calcd for [Pd(tn)$_2$]Cl$_2$=$C_6H_{20}N_4Cl_2Pd$: C, 22.13; H, 6.19; N, 17.21%.

[Pd(N)$_3$(O)]-type Complexes. *1) [Pd(gly)(NH$_3$)$_2$]ClO$_4$*: Silver perchlorate (246 mg) and freshly prepared silver oxide (140 mg) were successively added to a suspension of 250 mg of *cis*-[PdCl$_2$(NH$_3$)$_2$][7] in 10 cm^3 of water and the mixture was stirred at room temperature for 10 min in the dark. Immediately after removal of the silver chloride the filtrate was mixed with an aqueous solution (1 cm^3) of 89 mg of glycine, evaporated to *ca.* 4 cm^3 under reduced pressure, and chilled in an ice-bath. After 2 h lemon yellow crystals were collected, washed with cold water, and dried in air. Yield: 200 mg. Found: C, 7.73; H, 3.27; N, 13.34%. Calcd for $C_2H_{10}N_3ClO_6Pd$: C, 7.65; H, 3.21; N, 13.38%.

2) [Pd(gly)L]ClO$_4$ (L=en and tn): Each of these complexes was prepared by the method adopted for [Pd(*S*-ala)(*S*-pn)]ClO$_4$[2] but crystallized from a water–methanol medium. The crude product was recrystallized from warm water (*ca.* 60 °C). Yield: 55 (en) and 75% (tn complex). Found: C, 14.31; H, 3.60; N, 12.36%. Calcd for [Pd(gly)(en)]ClO$_4$=$C_4H_{12}N_3ClO_6Pd$: C, 14.13; H, 3.56; N, 12.36%. Found: C, 17.09; H, 4.03; N, 11.92%. Calcd for [Pd(gly)(tn)]ClO$_4$=$C_5H_{14}N_3ClO_6Pd$: C, 16.96; H, 3.99; N, 11.87%.

3) [Pd(β-ala)L]ClO$_4$ (L=en and tn) and [Pd(N-Megly)(en)]-

ClO$_4$: These complexes were prepared and crystallized in the same way as for [Pd(*S*-ala)(*S*-pn)]ClO$_4$.[2] The β-ala complexes were recrystallized from warm water, by adding acetone if necessary. Yield: 50 (en) and 70% (tn) for the β-ala complexes; and 90% for the *N*-Megly (=sarcosinato) complex. Found: C, 17.15; H, 4.06; N, 11.76%. Calcd for [Pd(β-ala)(en)]ClO$_4$=$\mathrm{C_5H_{14}N_3ClO_6Pd}$: C, 16.96; H, 3.99; N, 11.87%. Found: C, 19.68; H, 4.40; N, 11.37%. Calcd for [Pd(β-ala)(tn)]ClO$_4$=$\mathrm{C_6H_{16}N_3ClO_6Pd}$: C, 19.58; H, 4.38; N, 11.42%. Found: C, 17.09; H, 4.05; N, 11.85%. Calcd for [Pd(*N*-Megly)(en)]ClO$_4$=$\mathrm{C_5H_{14}N_3ClO_6Pd}$: C, 16.96; H, 3.99; N, 11.87%.

cis-*[Pd(N)$_2$(O)$_2$]-type Complexes.* *1) [Pd(CH$_3$CO$_2$)$_2$L] (L= en and tn)*: Each of these complexes was prepared by the same method as for [Pd(CH$_3$CO$_2$)$_2$(*S*-pn)][2] but crystallized from a water–acetone medium. Yield: 75—80%. Found: C, 24.19; H, 5.21; N, 9.37%. Calcd for [Pd(CH$_3$CO$_2$)$_2$(en)]·0.75H$_2$O= $\mathrm{C_6H_{15.5}N_2O_{4.75}Pd}$: C, 24.17; H, 5.24; N, 9.40%. Found: C, 26.57; H, 5.74; N, 8.55%. Calcd for [Pd(CH$_3$CO$_2$)$_2$(tn)]·H$_2$O=$\mathrm{C_7H_{18}N_2O_5Pd}$: C, 26.55; H, 5.73; N, 8.85%.

*2) [Pd(ox)L] (L=*rac*-pn and tn)*: These complexes were obtained by the reaction of [PdCl$_2$L] with silver oxalate,[2] in an 85—90% yield. Found: C, 22.36; H, 3.75; N, 10.44%. Calcd for [Pd(ox)(*rac*-pn)]=$\mathrm{C_5H_{10}N_2O_4Pd}$: C, 22.36; H, 3.75; N, 10.43%. Found: C, 22.37; H, 3.76; N, 10.46%. Calcd for [Pd(ox)(tn)]=$\mathrm{C_5H_{10}N_2O_4Pd}$: C, 22.36; H, 3.75; N, 10.43%.

3) [Pd(ox)(en)] and [Pd(mal)L] (L=cn, rac*-pn, and tn)*: These complexes were prepared by the method adopted for [Pd(mal)(*S*-pn)][2]. Yield: 70—85%. Found: C, 18.84; H, 3.21; N, 10.97%. Calcd for [Pd(ox)(en)]=$\mathrm{C_4H_8N_2O_4Pd}$: C, 18.87; H, 3.17; N, 11.01%. Found: C, 22.29; H, 3.78; N, 10.31%. Calcd for [Pd(mal)(en)]=$\mathrm{C_5H_{10}N_2O_4Pd}$: C, 22.36% H, 3.75; N, 10.43%. Found: C, 25.56; H, 4.28; N, 9.90%. Calcd for [Pd(mal)(*rac*-pn)]=$\mathrm{C_6H_{12}N_2O_4Pd}$: C, 25.50; H, 4.28; N, 9.91%. Found: C, 24.96; H, 4.44; N, 9.72%. Calcd for [Pd(mal)(tn)]·0.33H$_2$O=$\mathrm{C_6H_{12.66}N_2O_{4.33}Pd}$: C, 24.98; H, 4.42; N, 9.71%. The complexes [Pd(ox)(en)] and [Pd(mal)(en)] are almost insoluble in water.

4) [Pd(mal)(NH$_3$)$_2$]: A suspension of 200 mg of *cis*-[PdCl$_2$(NH$_3$)$_2$] in 6 cm^3 of water was stirred with 225 mg of freshly prepared silver oxide for 10 min at room temperature. After removal of the silver chloride the filtrate was evaporated to *ca.* 4 cm^3 under reduced pressure and mixed with an aqueous solution (1.5 cm^3) of 98 mg of malonic acid. The reaction mixture was allowed to stand at room temperature to give light orange crystals, which were washed with cold water and methanol and dried *in vacuo*. Yield: 180 mg. Found: C, 14.56; H, 3.47; N, 11.02%. Calcd for [Pd(mal)(NH$_3$)$_2$]·0.5H$_2$O=$\mathrm{C_3H_9N_2O_{4.5}Pd}$: C, 14.33; H, 3.61; N, 11.14%. This complex is insoluble in water without decomposition.

5) [Pd(ox)L$_2$] (L=NH$_3$, CH$_3$NH$_2$, and (CH$_3$)$_2$NH): These complexes were prepared from *cis-* or *trans*-[PdCl$_2$L$_2$][1] in the same manner as in 4). Yield: 75—85%. Found: C, 10.20; H, 2.82; N, 11.64%. Calcd for [Pd(ox)(NH$_3$)$_2$]·0.5H$_2$O=$\mathrm{C_2H_7N_2O_{4.5}Pd}$: C, 10.11; H, 2.97; N, 11.79%. Found: C, 17.44; H, 4.25; N, 9.95%. Calcd for [Pd(ox)(CH$_3$NH$_2$)$_2$]·H$_2$O=$\mathrm{C_4H_{12}N_2O_5Pd}$: C, 17.50; H, 4.41; N, 10.20%. Found: C, 22.22; H, 5.57; N, 8.59%. Calcd for [Pd(ox){(CH$_3$)$_2$NH}$_2$]·2H$_2$O=$\mathrm{C_6H_{18}N_2O_6Pd}$: C, 22.48; H, 5.66; N, 8.74%. Every complex is insoluble in water.

6) [Pd$_2$(μ-OH)$_2$L$_2$](ClO$_4$)$_2$ (L=en and tn): An aqueous solution containing each of these complexes was prepared in the same way as for [Pd$_2$(μ-OH)$_2$(*S*-pn)$_2$](ClO$_4$)$_2$.[2] The en complex was crystallized by mixing the concentrated solution with methanol-free acetone (because alcohols reduce the complex to deposit palladium metal), and the tn complex by evaporating and cooling the solution. Yield: 65% for both complexes. Found: C, 8.73; H, 3.29; N, 9.52%. Calcd for [Pd$_2$(μ-OH)$_2$(en)$_2$](ClO$_4$)$_2$=$\mathrm{C_4H_{18}N_4Cl_2O_{10}Pd_2}$: C, 8.49; H, 3.21; N, 9.90%. Found: C, 12.28; H, 3.75; N, 9.38%. Calcd for [Pd$_2$(μ-OH)$_2$(tn)$_2$](ClO$_4$)$_2$=$\mathrm{C_6H_{22}N_4Cl_2O_{10}Pd_2}$: C, 12.13; H, 3.73; N, 9.43%. The en complex is less stable than the corresponding *S*-pn one and decomposes in a basic aqueous solution, whereas the tn complex is more stable than the latter.

[Pd(N)(O)$_3$]-type Complexes. *1) K[Pd(CH$_3$CO$_2$)$_2$(gly)]*: The starting material K[PdCl$_2$(gly)] was prepared in the same way as for the corresponding *S*-ala complex.[8] Found: C, 7.88; H, 1.95; N, 4.58%. Calcd for K[PdCl$_2$(gly)]·H$_2$O=$\mathrm{C_2H_6NCl_2O_3KPd}$: C, 7.79; H, 1.96; N, 4.54%. The electronic absorption (AB) and MCD data in a 0.20 M KCl aqueous solution (1 M=1 mol dm^{-3}) are as follows in $\sigma_{\mathrm{max}}/10^3\,\mathrm{cm^{-1}}(\varepsilon/\mathrm{mol^{-1}\,dm^3\,cm^{-1}})$ and $\sigma_{\mathrm{ext}}/10^3\,\mathrm{cm^{-1}}\,(\Delta\varepsilon_{\mathrm{M}}/\mathrm{mol^{-1}\,dm^3\,cm^{-1}\,T^{-1}})$, respectively; AB: 19.6sh (13), 25.28 (312) [$\Delta\sigma^-$=2.56 and $\Delta\sigma^+$=2.63],[9] 37.8sh (1900), and 46.23 (19900) and MCD: 23.6 (+0.023), 26.8 (−0.027), 37.1 (+0.23), and 44.0 (−0.6).

The crude product which was obtained by the same method as for K[Pd(CH$_3$CO$_2$)$_2$(*S*-ala)][2] was considerably contaminated with bis(glycinato)palladium(II), and could not be purified by repeated recrystallizations from water–acetone. Orange-brown crystals deposited in the second recrystallization were mechanically separated from faint yellow needles [Pd(gly)$_2$]. Yield: 15%. Found: C, 21.45; H, 3.00; N, 4.17%. Calcd for $\mathrm{C_6H_{10}NO_6KPd}$: C, 21.34; H, 2.98; N, 4.15%.

2) K[Pd(mal)(gly)]: This complex was prepared and separated in a manner similar to that in 1). Yield: 30%. Found: C, 18.52; H, 1.94; N, 4.32%. Calcd for $\mathrm{C_5H_6NO_6KPd}$: C, 18.67; H, 1.88; N, 4.35%.

3) K[Pd(ox)(β-ala)]: The calculated quantity of a 1 M KOH aqueous solution was added drop by drop to an aqueous suspension containing equimolar amounts of palladium chloride and β-alanine, with stirring at *ca.* 45 °C. After continuous stirring a small amount of undissolved material was filtered off, and the filtrate was concentrated and mixed with acetone. The crude product K[PdCl$_2$(β-ala)] was recrystallized from water–acetone below 50 °C.[10] Found: C, 12.02; H, 2.04; N, 4.66%. Calcd for K[PdCl$_2$(β-ala)]=$\mathrm{C_3H_6NCl_2O_2KPd}$: C, 11.83; H, 1.99; N, 4.60%. The AB and MCD data in 0.20 M KCl are as follows in the same format as in 1); AB: 20.0sh (12), 25.66 (360) [$\Delta\sigma^-$=2.23 and $\Delta\sigma^+$=2.50], 38.4sh (2800), and 46.60 (17300) and MCD: 20 (+0.0008), 24.1 (+0.015), 27.3 (−0.027), 38.3 (+0.26), and 45.8 (−0.41).

An aqueous solution (20 cm^3) containing K[PdCl$_2$(β-ala)] (600 mg) and oxalic acid dihydrate (250 mg) was stirred with freshly prepared silver oxide (460 mg) for 10 min at room temperature. After removal of the silver chloride the filtrate was evaporated to *ca.* 4 cm^3. The product separated was dissolved again in the mother liquor at 50 °C and the resulting solution was allowed to stand at room temperature. Orange crystals were collected after 4 h, washed with a cold mixture of water–acetone, and dried *in vacuo*. Yield: 120 mg. Found: C, 18.59; H, 1.91; N, 4.27%. Calcd for $\mathrm{C_5H_6NO_6KPd}$: C, 18.67; H, 1.88; N, 4.35%. Further crops obtained from the mother liquor were contaminated with bis(oxalato)palladium(II) and could not be purified perfectly by recrystallization.

4) K[Pd(mal)(β-ala)]: This complex was prepared in the same manner as in 3), but crystallized from a more concentrated solution. Although the crude product was contaminated with a small amount of [Pd(β-ala)$_2$], it was purified twice by recrystallization from warm water–acetone. Yield: 40%. Found: C, 20.23; H, 2.94; N, 3.94%. Calcd for K[Pd(mal)(β-ala)]·H$_2$O=$\mathrm{C_6H_{10}NO_7KPd}$: C, 20.38; H, 2.85; N, 3.96%.

[Pd(O)$_4$]-type Complexes. The complexes K$_2$[Pd(ox)$_2$] and K$_2$[Pd(mal)$_2$] were prepared by a method similar to that reported for K$_2$[Pd(ox)$_2$],[11] but the number of water of crystallization was different from the literature values.[11–13]

Found: C, 12.09; H, 1.00%. Calcd for $K_2[Pd(ox)_2]\cdot 2H_2O$=$C_4H_4O_{10}K_2Pd$: C, 12.11; H, 1.02%. Found: C, 16.20; H, 2.29%. Calcd for $K_2[Pd(mal)_2]\cdot 3H_2O$=$C_6H_{10}O_{11}K_2Pd$: C, 16.28; H, 2.28%. The corresponding platinum(II) complexes, which were prepared for the purpose of comparison, turned out to have analogous compositions (Found: C, 9.99; H, 0.85%. Calcd for $K_2[Pt(ox)_2]\cdot 2H_2O$=$C_4H_4O_{10}K_2Pt$: C, 9.90; H, 0.83%. Found: C, 13.63; H, 1.95%. Calcd for $K_2[Pt(mal)_2]\cdot 3H_2O$=$C_6H_{10}O_{11}K_2Pt$: C, 13.56; H, 1.90%).

Measurements. Electronic absorption and MCD spectra were recorded with the same apparatus and in the same manner as described elsewhere.[3] Unless otherwise noted, all the measurements were made in aqueous solutions at room temperature. CD spectra were measured in our previous work.[2]

Results and Discussion

Synthesis. All the mixed-ligand palladium(II) complexes isolated in the present work were synthesized on the basis of the principle that a ligand with higher affinity for palladium(II) ion is made to coordinate in preference to a ligand with lower affinity.[2] However, disproportionation reactions were observed in the course of the synthesis of $[Pd(N)_3(O)]$- and $[Pd(N)(O)_3]$-type complexes, particularly in the latter. These complexes were usually contaminated with the corresponding bis(amino carboxylato) complexes, but $K[Pd(ox)(\beta\text{-ala})]$ was with the bis(oxalato) complex. The $[Pd(N)_3(O)]$-type complexes can be purified by recrystallization, whereas the $[Pd(N)(O)_3]$-type ones generally can not because a disproportionation reaction further proceeds during the course of recrystallization. The pure products of the latter type could be obtained only by careful crystallization under a mild condition followed by a mechanical separation. Although most of the complexes with every combination of the ligands were successfully isolated, the complexes $[Pd(tn)(NH_3)_2]Cl_2$, $[Pd(\beta\text{-ala})(NH_3)_2]ClO_4$, $K[Pd(ox)(gly)]$, and $K[Pd(CH_3CO_2)_2(\beta\text{-ala})]$ as well as mixed-ligand $[Pd(O)_4]$-type complexes could not be obtained.[14] As noticed easily, three of these complexes contain one six-membered chelate ring and two unidentate ligands. On the contrary, similar but neutral complexes, $[Pd(mal)(NH_3)_2]$ and $[Pd(CH_3CO_2)_2(tn)]$, could be isolated. This seems to be ascribed to the low solubilities of the mixed-ligand complexes relative to those of the disproportionation products.

The mixed-ligand complexes with en or gly are more labile than the corresponding complexes with *S*-pn or *S*-ala, judging from the degree of the disproportionation observed in the synthesis or recrystallization. This may be attributable to high flexibility of an en or gly chelate ring over an *S*-pn or *S*-ala one, but the following observations can not be explained so easily. The mixed-ligand complexes with tn or β-ala are also more labile than those with *S*-pn or *S*-ala when the remaining coordination sites are occupied by an *N,N*- or *N,O*-ligand, whereas they are comparable or more stable when the sites are occupied by an *O,O*- or two *O*-ligands.

MCD Spectra. *1) $[Pd(N)_4]$-type Complexes*: Figure 1 shows the absorption and MCD spectra of typical $[Pd(N)_4]$-type complexes together with the CD spectra of the corresponding optically active complexes. For convenience these spectra are divided into three regions: spin-forbidden d-d, spin-allowed d-d, and charge transfer (CT) regions (Tables 1 and 2). Each of the MCD spectra shows a positive band and a dispersion comprising a positive and a negative lobe in the spin-forbidden and -allowed d-d regions, respectively. The dispersion changes sign at 2—3×10³ cm⁻¹ lower energy than the peak position of the main negative CD band (*ca.* 35×10³ cm⁻¹), originating primarily from the $^1E_g \leftarrow {}^1A_{1g}$ transition (D_{4h}),[2] of the corresponding optically active complexes. The negative lobe lies at energies only by 0.2—0.5×10³ cm⁻¹ higher than the main CD band; and the positive lobe occurs at almost the same energy as the positive CD maximum of $[Pd(S\text{-pn})(tn)]^{2+}$ (31.4×10³ cm⁻¹), which has been assigned to the $^1A_{2g} \leftarrow {}^1A_{1g}$ transition (D_{4h}).[2] These facts suggest that the possible A term based on the $^1E_g \leftarrow {}^1A_{1g}$ transition does not contribute so significantly to the dispersion. Therefore, it is reasonable to consider, in combination with the information from the CD spectra,[2] that the positive lobe of the dispersion is mainly composed of a negative B term assigned to the $^1A_{2g} \leftarrow {}^1A_{1g}$ transition and that the large negative lobe is a composite of two positive B terms ascribed to the ^1E_g and $^1B_{1g} \leftarrow {}^1A_{1g}$ transitions (D_{4h}). The same assignment is appropriate for the *N,N*-Et_2en complexes (Fig. 2).

The MCD spectra have various features in the CT region, depending on the kind of the ligands. Namely, the complexes $[Pd(NH_3)_4]^{2+}$, $[Pd(tn)_2]^{2+}$, and $[Pd(en)_2]^{2+}$ exhibit a weak positive, an intense positive, and a medium negative band, respectively; however, an additivity holds qualitatively for the MCD spectra of

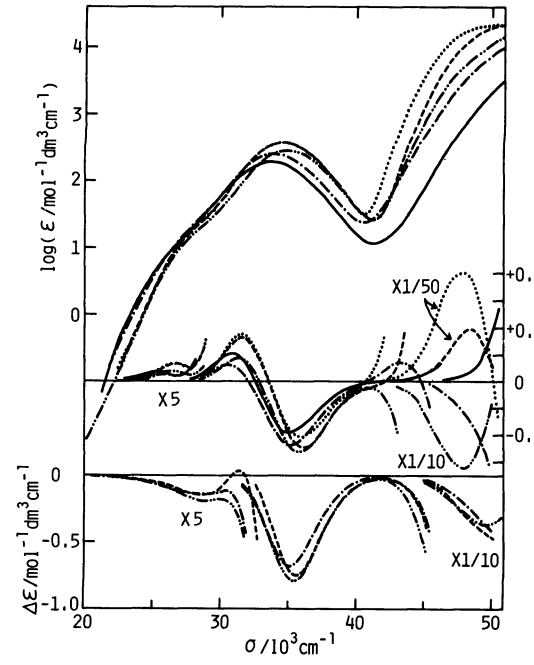

Fig. 1. Absorption and MCD spectra of $[Pd(NH_3)_4](ClO_4)_2$ (——), $[Pd(en)(NH_3)_2]Cl_2$ (—·—), $[Pd(en)_2]Cl_2$ (—··—), $[Pd(en)(tn)]Cl_2$ (------), and $[Pd(tn)_2]Cl_2$ (······); and CD spectra of $[Pd(S\text{-pn})(NH_3)_2]Cl_2$ (—·—), $[Pd(S\text{-pn})(en)]Cl_2$ (—··—), and $[Pd(S\text{-pn})(tn)]Cl_2$ (------).

TABLE 1. ABSORPTION DATA[a] OF $[Pd(N)_4]$-TYPE COMPLEXES $[Pd(L_1)(L_2)]Cl_2 \cdot nH_2O$

$(L_1)(L_2)$	n	$\sigma_{max}/10^3\,cm^{-1}(\varepsilon/mol^{-1}\,dm^3\,cm^{-1})$			
		Spin-forbidden d-d	Spin-allowed d-d	Charge transfer	
$(NH_3)_4$[b]	0	27.8 sh(19)	33.68(193)		
$(NH_3)_4$[b,c]	0	27.6 sh(15)	33.67(211)		
$(en)(NH_3)_2$	0	28.4 sh(26)	34.03(253)		
$(en)_2$	0	28.8 sh(22)	34.83(286)		
(en)(tn)	0	28.6 sh(24)	34.60(374)		
$(tn)_2$	0	28.6 sh(23)	34.60(378)	50.76(20900)	
(*N,N*-Et_2en)(en)	2	28.2 sh(53)	34.13(395)	49.88(16000)	
(*N,N*-Et_2en)(tn)	1	28.0 sh(41)	33.90(477)	48.29(18800)	
(*N,N*-Et_2en)$_2$[d]	0	27.4 sh(42)	33.61(572)	44.25(14400)	48.2 sh(11600)
(*N,N,C,C*-Me_4en)$_2$[d]	2	27.6 sh(41)	33.68(596)	44.44(15300)	48.2 sh(12400)

a) sh: shoulder (ε is for the value σ given). b) Perchlorate. c) In acetonitrile. d) Another band was observed at *ca.* $22 \times 10^3\,cm^{-1}$ as a shoulder.

TABLE 2. MCD DATA[a] OF $[Pd(N)_4]$-TYPE COMPLEXES $[Pd(L_1)(L_2)]Cl_2$[b]

$(L_1)(L_2)$	$\sigma_{ext}/10^3\,cm^{-1}(\Delta\varepsilon_M/mol^{-1}\,dm^3\,cm^{-1}\,T^{-1})$		
	Spin-forbidden d-d	Spin-allowed d-d	Charge transfer
$(NH_3)_4$[c]	25.3(+0.0008)	30.8(+0.011)	
	26.8 m	35.0(−0.019)	
$(NH_3)_4$[c, d]	25.3(+0.0007)	30.6(+0.012)	46.5(−0.002)
	26.8 m	34.9(−0.021)	
$(en)(NH_3)_2$	26.0(+0.0006)	30.5(+0.006)	43.3(+0.008)
	26.9 m	35.2(−0.024)	
$(en)_2$	26.3(+0.0008)	31.3(+0.009)	48.0(−0.32)
	27.7 m	35.8(−0.026)	
(en)(tn)	26.8(+0.0014)	31.6(+0.016)	48.4(+0.93)
	27.8 m	36.1(−0.024)	
$(tn)_2$	26.6(+0.0014)	31.6(+0.018)	47.8(+2.0)
	27.7 m	36.0(−0.020)	
(*N,N*-Et_2en)(en)	26.2(+0.0013)	30.6(+0.011)	45.7(−0.28)
	27.5 m	35.2(−0.033)	
(*N,N*-Et_2en)(tn)	25.9(+0.0011)	30.8(+0.012)	46.4(+0.56)
	27.4 m	35.4(−0.026)	
(*N,N*-Et_2en)$_2$	25.5(+0.0019)	29.7(+0.011)	43.2(−0.26)
	26.5 m	34.4(−0.038)	48.9(+0.22)
(*N,N,C,C*-Me_4en)$_2$	25.6(+0.0017)	29.9(+0.011)	43.1(−0.38)
	26.6 m	34.5(−0.039)	48.6(+0.35)

a) m; minimum of $|\Delta\varepsilon_M|$. b) Water of crystallization is omitted (See Table 1). c) Perchlorate. d) In acetonitrile.

the mixed-ligand complexes (Fig. 1). An analogous situation is also observed for the mixed-ligand *N,N*-Et_2en complexes. A positive and a negative A term are correlated with the CT absorption bands around $50 \times 10^3\,cm^{-1}$ in the complexes of en and tn, respectively (Fig. 2). We previously found that the complexes having two *N,N*-dialkylamino groups in positions trans to each other exhibited a splitting both in the absorption and CD bands which were assigned to Pd←N(σ) transitions.[2] The spectra of such complexes show a negative and a positive band corresponding to the two split components (Fig. 2). These two B terms may be considered as a pseudo A term.[15] The MCD spectrum of $[Pd(en)(NH_3)_2]^{2+}$ shows a weak positive band on the lower edge of the CT absorption band, and it is presumably attributed to an orbitally-forbidden CT transition.

2) $[Pd(N)_3(O)]$-type Complexes: The spectra of the complexes containing gly or *β*-ala are shown in Fig. 3 or 4, respectively, and the numerical data in Tables 3 and 4. The MCD spectra showed a single positive or a couple of + and − bands in the spin-forbidden d-d region. Taking into account the overlapping of the neighboring intense positive band, all the complexes are expected to have the two (+ and −) bands in the region. The minimum around $26 \times 10^3\,cm^{-1}$ is considered to be formed by such an undetectable negative band, and included in Table 4; the main CD band of spin-forbidden nature occurs at almost the same energy as the minimum (Figs. 3 and 4). Such a correspondance is also found in the $[Pd(N)_4]$-type complexes (Figs. 1 and 2; Table 2).

The MCD spectra in the spin-allowed d-d region of the $[Pd(gly)(N)_2]$-type complexes are very similar to those of the corresponding $[Pd(en)(N)_2]$-type complexes (Figs. 3 and 1). The MCD spectra of the

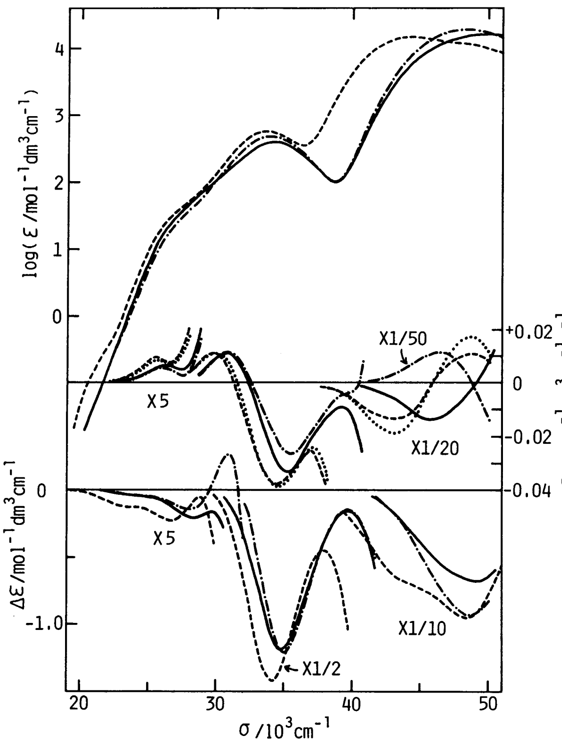

Fig. 2. Absorption and MCD spectra of [Pd(*N*,*N*-Et$_2$en)(en)]Cl$_2$ (——), [Pd(*N*,*N*-Et$_2$en)(tn)]Cl$_2$ (—·—), and [Pd(*N*,*N*-Et$_2$en)$_2$]Cl$_2$ (------); MCD spectrum of [Pd(*N*,*N*,*C*,*C*-Me$_4$en)$_2$]Cl$_2$ (······) (the absorption spectrum is almost identical with that of [Pd(*N*,*N*-Et$_2$en)$_2$]Cl$_2$); and CD spectra of [Pd(*N*^{1},*N*^{1}-Et$_2$-(*S*)-pn)(en)]Cl$_2$ (——), [Pd(*N*^{1},*N*^{1}-Et$_2$-(*S*)-pn)(tn)]Cl$_2$ (—·—), and [Pd(*N*^{1},*N*^{1}-Et$_2$-(*S*)-pn)$_2$]Cl$_2$ (------).

[Pd(β-ala)(N)$_2$]-type complexes in the same region do not largely differ from those of the corresponding gly complexes (Figs. 4 and 3). Thus, these MCD spectra can be interpreted in analogy with those of the [Pd(N)$_4$]-type complexes. The complexes containing tn exhibit larger intensity ratios of the positive to the negative lobe of the dispersion, $|\Delta\varepsilon_M(+)/\Delta\varepsilon_M(-)|$, than the corresponding en complexes. Moreover it is noteworthy that the ratio is closely related to the sign and intensity of the MCD band in 45—50×10^3 cm^{-1}: the complexes which exhibit an intense positive MCD in the CT region do also an intense positive MCD band in the spin-allowed d-d region, and the complexes with a negative band in the former region exhibit a weak positive band in the latter region (Figs. 2 and 3). This fact is proved to hold likewise for the complexes of the other types, implying the mixing of a CT excited state with a d-d vibronic excited state.

Again in the CT region, the [Pd(gly)(N)$_2$]-type complexes generally exhibit MCD features similar to those of the corresponding en complexes, except for the positive band at 43.3×10^3 cm^{-1} in [Pd(en)(NH$_3$)$_2$]$^{2+}$. On the other hand, [Pd(β-ala)(en)]$^+$ exhibits a unique pattern of −, +, and −, and [Pd(β-ala)(tn)]$^+$ a pattern characteristic of the complexes containing tn. These observations indicate that gly and en ligands make an almost equivalent contribution to the MCD in the region but that a β-ala has a greater influence on the MCD than an en but smaller than a tn.

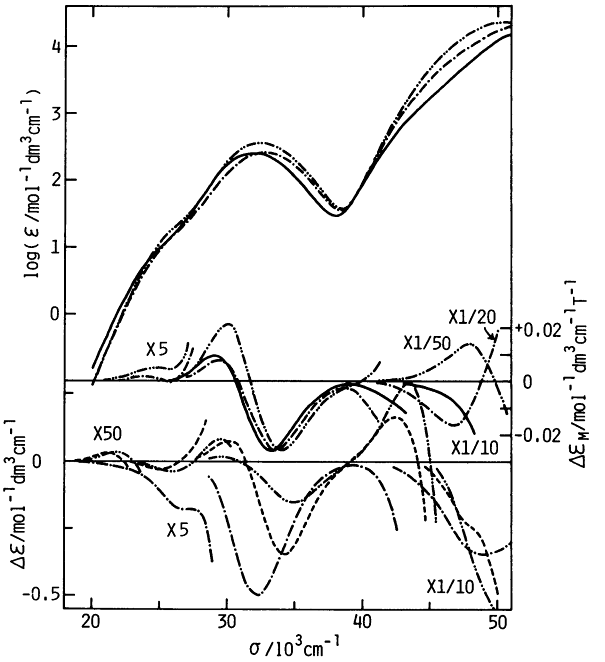

Fig. 3. Absorption and MCD spectra of [Pd(gly)L]ClO$_4$: L=(NH$_3$)$_2$ (——), L=en (—·—), and L=tn (—··—); and CD spectra of [Pd(gly)(*S*-pn)]ClO$_4$ (—·—), [Pd-(*S*-ala)(en)]ClO$_4$ (------), and [Pd(*S*-ala)(tn)]ClO$_4$ (—··—).

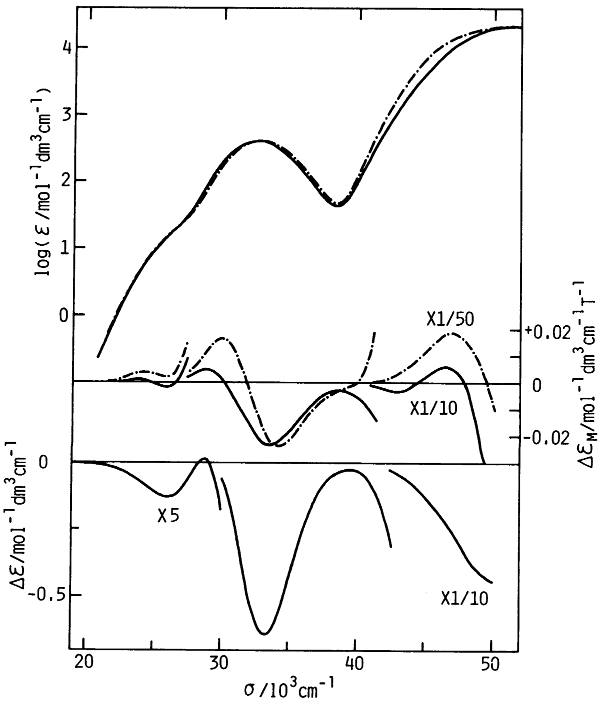

Fig. 4. Absorption and MCD spectra of [Pd(β-ala)L]ClO$_4$: L=en (——) and L=tn (—·—), and CD spectrum of [Pd(β-ala)(*S*-pn)]ClO$_4$ (——).

3) cis-[Pd(N)$_2$(O)$_2$]-type Complexes: The spectra of the complexes with this type are shown in Figs. 5—7, and the numerical data in Tables 5 and 6. The situation in the spin-forbidden d-d region is substantially the same as for the [Pd(N)$_3$(O)]- and [Pd(N)$_4$]-type complexes, but the negative MCD band in the higher energy side appears more explicitly. A comparison of the MCD spectrum of [Pd(ox)(*rac*-pn)] with the CD

Table 3. Absorption data[a] of $[Pd(N)_3(O)]$-type complexes $[Pd(L_1)(L_2)]ClO_4$

$(L_1)(L_2)$	$\sigma_{max}/10^3\,cm^{-1}(\varepsilon/mol^{-1}\,dm^3\,cm^{-1})$		
	Spin-forbidden d-d	Spin-allowed d-d	Charge transfer
$(gly)(NH_3)_2$	25.4 sh(12)	31.81(254)	44.5 sh
(gly)(en)	26.4 sh(19)	32.70(259)	
(gly)(tn)	26.4 sh(23)	32.35(360)	50.61(22700)
(β-ala)(en)	26.2 sh(17)	32.46(406)	51.28(20600)
(β-ala)(tn)	26.6 sh(21)	32.68(410)	51.63(21600)
(*N*-Megly)(en)	26.4 sh(22)	32.83(284)	51.41(22500)

a) sh: shoulder (ε is for the value σ given).

Table 4. MCD data[a] of $[Pd(N)_3(O)]$-type complexes $[Pd(L_1)(L_2)]ClO_4$

$(L_1)(L_2)$	$\sigma_{ext}/10^3\,cm^{-1}(\Delta\varepsilon_M/mol^{-1}\,dm^3\,cm^{-1}\,T^{-1})$		
	Spin-forbidden d-d	Spin-allowed d-d	Charge transfer
$(gly)(NH_3)_2$	24 sh(+0.0003)	28.9(+0.010) 33.2(−0.026)	
(gly)(en)	23.8(+0.0004) 25.8(−0.00004)	29.3(+0.008) 33.5(−0.026)	46.7(−0.33)
(gly)(tn)	24.7(+0.0010) 25.8 m	30.0(+0.021) 34.0(−0.026)	47.8(+0.70)
(β-ala)(en)	24 sh(+0.0002) 25.9(−0.0004)	28.8(+0.005) 33.5(−0.023)	42.8(−0.03) 46.6(+0.06)
(β-ala)(tn)	24.1(+0.0008) 26.0 m	29.9(+0.017) 34.1(−0.024)	46.9(+0.94)
(*N*-Megly)(en)	24.5(+0.0008) 25.9 m	29.3(+0.010) 33.5(−0.028)	46.2(−0.30)

a) sh: shoulder ($\Delta\varepsilon_M$ is for the value σ given); m: minimum of $|\Delta\varepsilon_M|$.

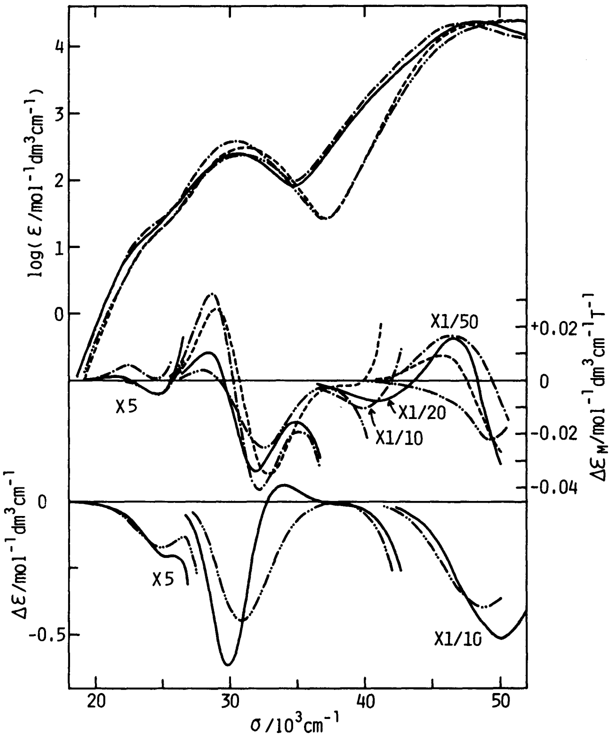

Fig. 5. Absorption and MCD spectra of [Pd(ox)(*rac*-pn)] (——), [Pd(ox)(tn)] (—·—), [Pd(mal)(*rac*-pn)] (—··—), and [Pd(mal)(tn)] (------); and CD spectra of [Pd(ox)(*S*-pn)] (——) and [Pd(mal)(*S*-pn)] (—··—).

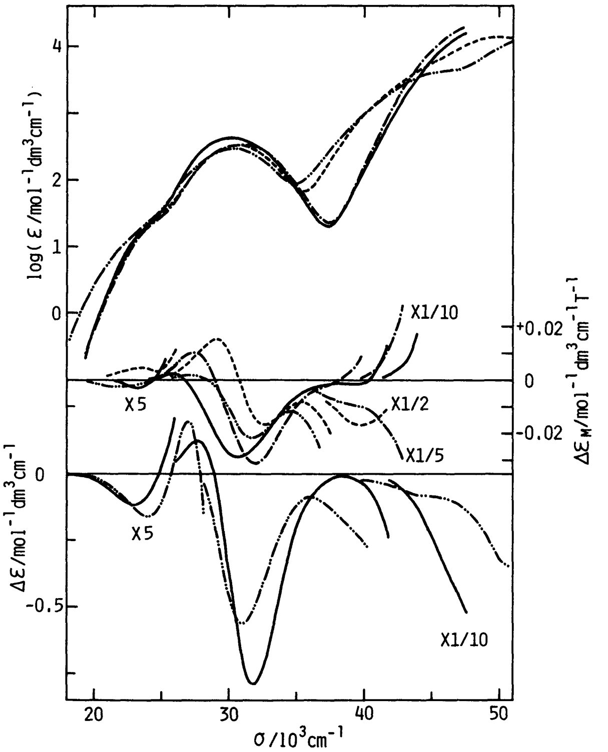

Fig. 6. Absorption and MCD spectra of $[Pd(CH_3CO_2)_2L]$ in 0.50 M CH_3CO_2Na: L=en (——) and L=tn (—·—), and $[Pd_2(\mu\text{-}OH)_2L_2](ClO_4)_2$ in H_2O: L=en (—··—) and L=tn (------); and CD spectra of $[Pd(CH_3CO_2)_2(S\text{-}pn)]$ in 0.50 M CH_3CO_2Na (——) and $[Pd_2(\mu\text{-}OH)_2(S\text{-}pn)_2](ClO_4)_2$ in H_2O (—··—).

one of [Pd(ox)(*S*-pn)] in the spin-allowed d-d region leads to the expectation that the A term based on the $^1E_g \leftarrow {}^1A_{1g}$ transition (D_{4h}) contributes to the dispersion of MCD more substantially than in the case of the [Pd(N)$_4$]- and [Pd(N)$_3$(O)]-type complexes (Fig. 5). The CD band at *ca.* 34×10^3 cm^{-1}, which was assigned to the $^1B_{1g} \leftarrow {}^1A_{1g}$ transition (D_{4h}),[2] is correlated to a positive B term included in the negative lobe of the dispersion. The intensity ratio, $|\Delta\varepsilon_M(+)/\Delta\varepsilon_M(-)|$, is determined primarily by the kind of the *N*-ligand as seen in the previous section and secondarily by that of the *O*-ligand: it decreases in the order of the ox, mal, and CH$_3$CO$_2$ complexes when compared within the complexes with the same *N*-ligand. No such regularity is found for the complexes with μ-hydroxo or aqua ligands. The complex [Pd(OH$_2$)$_2$(en)]$^{2+}$ is so unique among the series of the complexes studied here as to exhibit only a negative band in the MCD of the spin-allowed d-d region (Fig. 7). The MCD band lies at the lower energy side of the main CD band of [Pd(OH$_2$)$_2$(*S*-pn)]$^{2+}$; accordingly, a positive B term is expected for the $^1A_{2g} \leftarrow {}^1A_{1g}$ transition (D_{4h}) in this complex. The diacetato complex [Pd(CH$_3$CO$_2$)$_2$(en)] is similarly situated, although it exhibits a weak positive MCD band. The weak band is considered to be the remainder of the positive lobe of the minor negative A term based on the $^1E_g \leftarrow {}^1A_{1g}$ transition canceled by the positive B term on the $^1A_{2g} \leftarrow {}^1A_{1g}$ one.

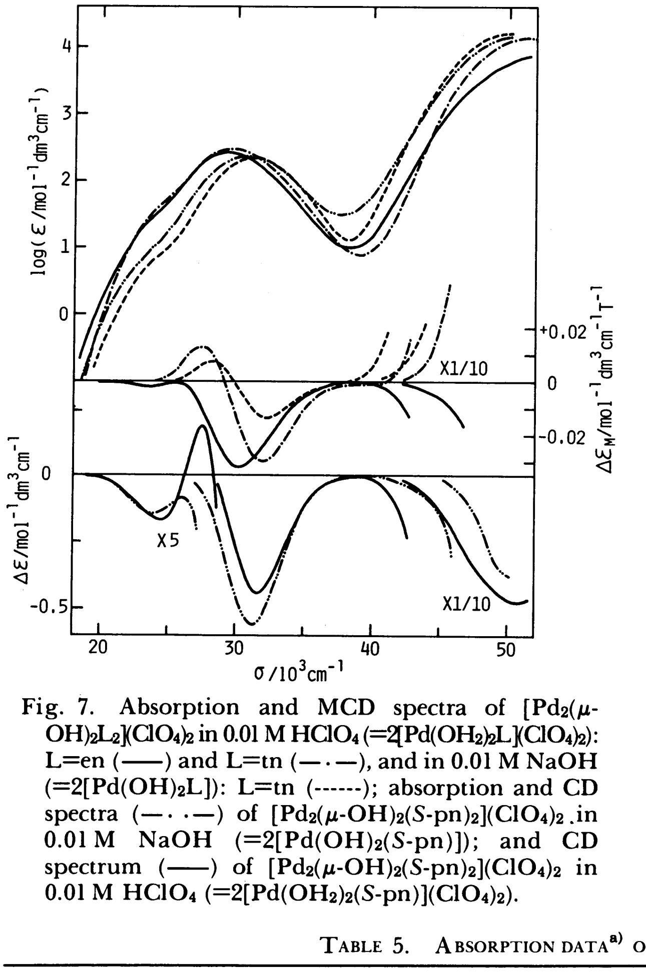

Fig. 7. Absorption and MCD spectra of [Pd$_2$(μ-OH)$_2$L$_2$](ClO$_4$)$_2$ in 0.01 M HClO$_4$ (=2[Pd(OH$_2$)$_2$L](ClO$_4$)$_2$): L=en (——) and L=tn (—·—), and in 0.01 M NaOH (=2[Pd(OH)$_2$L]): L=tn (------); absorption and CD spectra (—··—) of [Pd$_2$(μ-OH)$_2$(*S*-pn)$_2$](ClO$_4$)$_2$ in 0.01 M NaOH (=2[Pd(OH)$_2$(*S*-pn)]); and CD spectrum (——) of [Pd$_2$(μ-OH)$_2$(*S*-pn)$_2$](ClO$_4$)$_2$ in 0.01 M HClO$_4$ (=2[Pd(OH$_2$)$_2$(*S*-pn)](ClO$_4$)$_2$).

The MCD spectra in the CT region of the complexes with ox or mal are qualitatively additive with respect to the constituent ligands as noted in the [Pd(N)$_4$]-type complexes (Figs. 5, 1, and 9). This fact agrees with the expectation that two kinds of CT transitions, namely Pd←N(σ) and O(n, π, and/or σ), are present with small energy gaps. The absorption band which was observed as a shoulder around 42×10^3 cm^{-1} in the complexes with ox is readily assigned to the latter CT transitions, to which a positive B term corresponds. On the other hand, the CD spectra show no remarkable band in 35—45×10^3 cm^{-1}; this can be explained by the fact that an asymmetric center is present only in the *N*-ligand, if such a chirality is more effective in Pd←N than in Pd←O CT transitions. A similar spectral behavior has been observed also for [Pd(Cl)$_2$(N)$_2$]-type complexes.[1] Therefore, the CD bands at *ca.* 50×10^3 cm^{-1} are attributable primarily to Pd←N(σ) transitions (Fig. 5).

4) [Pd(N)(O)$_3$]-type Complexes: The absorption and MCD spectra of the complexes of this type are shown in Fig. 8 together with the CD spectra of the relating complexes with *S*-ala, and the numerical data in Tables 7 and 8. The MCD spectra of the complexes with gly are very similar to those of the corresponding en (or *rac*-pn) complexes of *cis*-[Pd(N)$_2$(O)$_2$]-type over the range 20—50×10^3 cm^{-1} (Figs. 8, 5, and 6). Thus, the MCD spectra of the former complexes can be interpreted in analogy with those of the latter. The MCD spectrum of [Pd(CH$_3$CO$_2$)$_2$(gly)]$^-$ supports the idea proposed be-

TABLE 5. ABSORPTION DATA[a] OF *cis*-[Pd(N)$_2$(O)$_2$]-TYPE COMPLEXES

Complex	σ_{max}/10^3 cm^{-1}(ε/mol^{-1} dm^3 cm^{-1})			
	Solvent	Spin-forbidden d-d	Spin-allowed d-d	Charge transfer
[Pd(CH$_3$CO$_2$)$_2$(en)]·0.75H$_2$O	0.50 M CH$_3$CO$_2$Na	24.2 sh(23)	30.11(430)	
[Pd(CH$_3$CO$_2$)$_2$(tn)]·H$_2$O	0.50 M CH$_3$CO$_2$Na	24.6 sh(24)	31.00(340)	
[Pd(ox)(*rac*-pn)]	H$_2$O	24.4 sh(19)	30.53(253)	48.08(23100)
[Pd(ox)(tn)]	H$_2$O	24.8 sh(25)	30.40(384)	47.17(21800)
[Pd(mal)(*rac*-pn)]	H$_2$O	24.8 sh(18)	31.00(240)	51.36(23700)
[Pd(mal)(tn)]·0.33H$_2$O	H$_2$O	25.2 sh(21)	31.14(311)	50.63(24400)
[Pd$_2$(μ-OH)$_2$(en)$_2$](ClO$_4$)$_2$[b]	H$_2$O	23.8 sh(21)	30.44(291)	45.5 sh(4100)
	0.01 M HClO$_4$	24.4 sh(37)	29.21(270)	
[Pd$_2$(μ-OH)$_2$(tn)$_2$](ClO$_4$)$_2$[b]	H$_2$O	24.4 sh(22)	30.71(332)	44 sh
				50.10(13700)
	0.01 M HClO$_4$	24.8 sh (53)	29.50(300)	51.49(13600)
	0.01 M NaOH	24.6 sh(9)	31.23(219)	

a) sh: shoulder (ε is for the value σ given). b) Molar absorption coefficient is based on palladium; another band was observed at *ca.* 39.5×10^3 cm^{-1} as a shoulder.

Table 6. MCD data[a)] of *cis*-$[Pd(N)_2(O)_2]$-type complexes

Complex	Solvent	$\sigma_{ext}/10^3\,cm^{-1}(\Delta\varepsilon_M/mol^{-1}\,dm^3\,cm^{-1}\,T^{-1})$ Spin-forbidden d-d	Spin-allowed d-d	Charge transfer
$[Pd(CH_3CO_2)_2(en)]\cdot 0.75H_2O$	0.50 M CH_3CO_2Na		25.9(+0.002)	
		23.2(−0.0006)	30.7(−0.029)	
$[Pd(CH_3CO_2)_2(tn)]\cdot H_2O$	0.50 M CH_3CO_2Na		27.4(+0.010)	
			31.9(−0.031)	
[Pd(ox)(*rac*-pn)]	H_2O	21.7 sh(+0.0003)	28.4(+0.011)	40.8(−0.15)
		24.6(−0.001)	31.9(−0.034)	46.5(+0.32)
[Pd(ox)(tn)]	H_2O	22.4(+0.0011)	28.6(+0.032)	39.9(−0.10)
		24.5 m	32.1(−0.041)	46.4(+0.83)
[Pd(mal)(*rac*-pn)]	H_2O		28.0(+0.004)	49.3(−1.1)
		24.7(−0.001)	32.5(−0.025)	
$[Pd(mal)(tn)]\cdot 0.33H_2O$	H_2O		29.0(+0.027)	45.7(+0.45)
			32.9(−0.035)	
$[Pd_2(\mu\text{-}OH)_2(en)_2](ClO_4)_2$[b)]	H_2O	21.7(−0.0005)	27.2(+0.002)	39.5 sh(−0.05)
			31.6(−0.022)	
	0.01 M $HClO_4$		25.6 m	
		23.6(−0.002)	30.2(−0.032)	
$[Pd_2(\mu\text{-}OH)_2(tn)_2](ClO_4)_2$[b)]	H_2O		29.0(+0.015)	39.7(−0.034)
		23.5(+0.0009)	32.6(−0.017)	
	0.01 M $HClO_4$		27.4(+0.013)	
			32.0(−0.030)	
	0.01 M NaOH		28.2(+0.007)	
			32.2(−0.014)	

a) sh: shoulder ($\Delta\varepsilon_M$ is for the value σ given); m: minimum of $|\Delta\varepsilon_M|$. b) $\Delta\varepsilon_M$ is based on palladium.

fore that the vicinal CD contribution by *S*-ala exhibits a dispersion pattern of + and − for the ${}^1E_g \leftarrow {}^1A_{1g}$ transition (D_{4h}).[2)] The MCD spectra of the two complexes with *β*-ala are similar to that of $[Pd(\beta\text{-}ala)(en)]^+$ in the d-d region, particularly in the intensity ratio $|\Delta\varepsilon_M(+)/\Delta\varepsilon_M(-)|$, and showed a composite of the patterns characteristic of the constituent ligands in the CT region (Figs. 8 and 4).

5) $[Pd(O)_4]$-type Complexes: The absorption and MCD spectra are shown in Fig. 9 and the numerical data in Tables 7 and 8. The MCD curves in the d-d region of $[Pd(ox)_2]^{2-}$ and $[Pd(mal)_2]^{2-}$ are very similar to each other, although the intensity for the former complex is about a half of that for the latter. Considering only coordinating atoms, the complexes of this type can be approximated by a D_{4h} symmetry; nevertheless the contribution of the A term based on the ${}^1E_g \leftarrow {}^1A_{1g}$ transition is considered to be small from the MCD features. This situation is similar to that in the $[Pd(N)_4]$-type complexes.

The MCD spectrum of $[Pd(ox)_2]^{2-}$ showed four bands in the CT region. The lowest-energy band, which was observed only as a shoulder, corresponds to the absorption band (shoulder) at $32.8\times10^3\,cm^{-1}$. Neither the MCD nor the absorption band corresponding to the above respective band was observable in the complexes containing only one ox ligand because of the relatively high intensities of the neighboring bands. The three higher-energy bands are familiar in the complexes with ox (See also Figs. 5 and 8). The MCD spectrum of $[Pd(mal)_2]^{2-}$ showed two bands in the CT region; a positive B term and a positive A term correspond to the absorption bands at 44.5 and $48.5\times10^3\,cm^{-1}$, respectively.

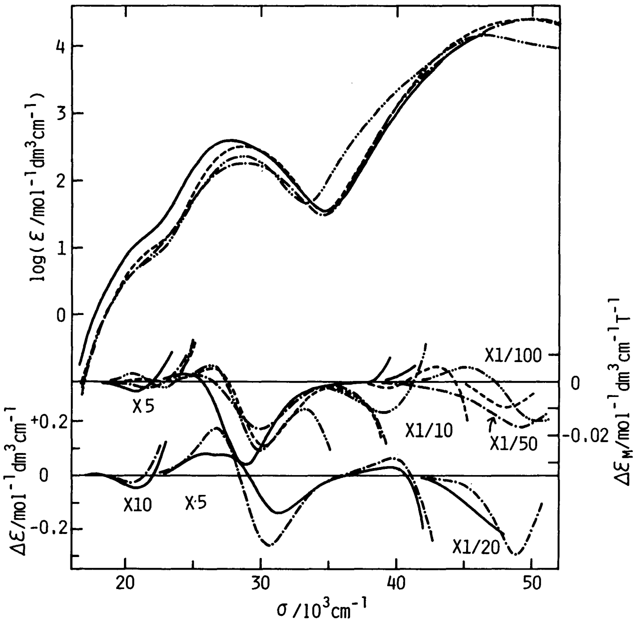

Fig. 8. Absorption and MCD spectra of $K[Pd(CH_3CO_2)_2(gly)]$ in 0.50 M CH_3CO_2Na (——), K[Pd(mal)(gly)] in H_2O (—·—), K[Pd(ox)(*β*-ala)] in H_2O (—· ·—), and K[Pd(mal)(*β*-ala)] in H_2O (------); and CD spectra of $K[Pd(CH_3CO_2)_2(S\text{-}ala)]$ in 0.50 M CH_3CO_2Na (——) and K[Pd(mal)(*S*-ala)] in H_2O (—·—).

Ligand-field Absorption Spectra. Each absorption spectrum of the $[Pd(N)_n(O)_{4-n}]$-type complexes is

TABLE 7. ABSORPTION DATA[a] OF $[Pd(N)(O)_3]$- AND $[Pd(O)_4]$-TYPE COMPLEXES

Complex	$\sigma_{max}/10^3\,cm^{-1}(\varepsilon/mol^{-1}\,dm^3\,cm^{-1})$			
	Spin-forbidden d-d	Spin-allowed d-d	Charge transfer	
$K[Pd(CH_3CO_2)_2(gly)]$[b]	21.6 sh(16)	27.77(402)		
K[Pd(mal)(gly)]	22.0 sh(9)	28.79(184)	44 sh	50.06(25200)
K[Pd(ox)(β-ala)]	21.8 sh(11)	28.58(372)	39.5 sh	46.45(22200)
$K[Pd(mal)(\beta\text{-ala})]\cdot H_2O$	22.4 sh(11)	28.69(326)		49.44(24900)
$K_2[Pd(ox)_2]\cdot 2H_2O$[c]	19.2 sh(4)	26.31(106)	37.5 sh(3400)	44.39(24100)
$K_2[Pd(mal)_2]\cdot 3H_2O$	20.4 sh(7)	26.99(164)	44.5 sh	48.53(27800)

a) sh: shoulder (ε is for the value σ given). b) In 0.50 M CH_3CO_2Na. c) Another band was observed at *ca.* $32.8\times 10^3\,cm^{-1}$ (ε=150) as a shoulder.

TABLE 8. MCD DATA OF $[Pd(N)(O)_3]$- AND $[Pd(O)_4]$-TYPE COMPLEXES

Complex	$\sigma_{ext}/10^3\,cm^{-1}(\Delta\varepsilon_M/mol^{-1}\,dm^3\,cm^{-1}\,T^{-1})$		
	Spin-forbidden d-d	Spin-allowed d-d	Charge transfer
$K[Pd(CH_3CO_2)_2(gly)]$[a]		24.4(+0.003)	
	20.7(−0.0007)	28.8(−0.031)	
K[Pd(mal)(gly)]		25.2(+0.0025)	49.2(−0.85)
	21.6(−0.0004)	30.0(−0.018)	
K[Pd(ox)(β-ala)]	20.4(+0.0006)	26.2(+0.0061)	39.0(−0.12)
	22.8(−0.0004)	29.9(−0.026)	45.1(+0.55)
			50.6(−1.5)
$K[Pd(mal)(\beta\text{-ala})]\cdot H_2O$	21.3(+0.0002)	26.4(+0.0050)	39.3(−0.02)
		30.2(−0.024)	42.9(+0.06)
			48.1(−1.0)
$K_2[Pd(ox)_2]\cdot 2H_2O$[b]		23.3(+0.0029)	36.9(−0.19)
	18.7(−0.0002)	27.1(−0.011)	43.8(+0.54)
			49.3(−0.90)
$K_2[Pd(mal)_2]\cdot 3H_2O$		24.7(+0.0067)	46.7(−1.1)
	20.2(−0.0003)	28.5(−0.020)	

a) In 0.50 M CH_3CO_2Na. b) Another band was observed at *ca.* $32.5\times 10^3\,cm^{-1}$ ($\Delta\varepsilon_M$=−0.02) as a shoulder.

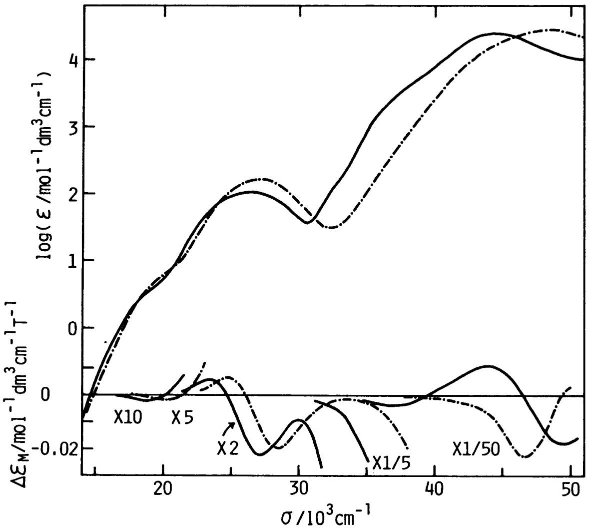

Fig. 9. Absorption and MCD spectra of $K_2[Pd(ox)_2]$ (——) and $K_2[Pd(mal)_2]$ (—·—).

composed of an unsymmetrical broad band and a lower-lying shoulder in the d-d transition region, and these bands are roughly assigned to a spin-allowed and a spin-forbidden band, respectively. The former band will be described in detail and discussed briefly hereafter. We previously demonstrated that such an unsymmetrical band could be characterized by the half-value-width parameters and the unsymmetry parameter.[1] The parameters are listed in Table 9 for the complexes studied here.

Figure 10 represents the complexes together with the relating optically active complexes[2] as a function of the molar absorption coefficient of the absorption peak and the half-value width $\Delta\sigma_{1/2}$; moreover it shows the approximate band area, which is proportional to the oscillator strength. The $[Pd(N)_4]$-type complexes composed of ammine, en (or *S*-pn) and/or tn are classified into four groups, *i.e.*, a tetraammine complex, diammine(five-membered chelate) complexes, bis(five-membered chelate) complexes, and tn-containing complexes; the half-value width decreases and the band area increases in this order. A similar behavior is also found among the $[Pd(N)_4]$-type complexes containing *N,N*-diethylethylene(or propylene)diamine. The $[Pd(N)_3(O)]$-type complexes can be classified into three groups: complexes containing no six-membered chelates, complexes composed of a five-membered N–O and a six-membered N–N chelate, and complexes containing a six-membered N–O chelate. Thus the complexes with β-ala form a single group in Fig. 10 irrespective of the sizes of the accompanying diamines, and this situation is very similar to that found for the $[Pd(N)_4]$-type complexes with tn.

TABLE 9. BAND SHAPE PARAMETERS FOR THE SPIN-ALLOWED d-d BAND OF $[Pd(N)_n(O)_{4-n}]$-TYPE COMPLEXES (n=0—4)

Complex	$\Delta\sigma^-$ a)	$\Delta\sigma^+$ a)	$\Delta\sigma_{1/2}$ a)	Unsymmetry parameter b)
	10^3 cm^{-1}	10^3 cm^{-1}	10^3 cm^{-1}	
$[Pd(NH_3)_4]^{2+}$	2.73	2.88	5.61	2.7
$[Pd(NH_3)_4]^{2+}$c)	2.50	2.71	5.22	4.0
$[Pd(en)(NH_3)_2]^{2+}$	2.73	2.79	5.52	1.1
$[Pd(en)_2]^{2+}$	2.53	2.77	5.30	4.5
$[Pd(en)(tn)]^{2+}$	2.51	2.72	5.23	4.0
$[Pd(tn)_2]^{2+}$	2.48	2.68	5.16	3.9
$[Pd(N,N\text{-}Et_2en)(en)]^{2+}$	2.75	2.75	5.50	0.0
$[Pd(N,N\text{-}Et_2en)(tn)]^{2+}$	2.57	2.69	5.26	2.3
$[Pd(gly)(NH_3)_2]^+$	2.53	2.84	5.38	5.8
$[Pd(gly)(en)]^+$	2.70	2.77	5.47	1.3
$[Pd(gly)(tn)]^+$	2.48	2.81	5.29	6.2
$[Pd(\beta\text{-}ala)(en)]^+$	2.42	2.66	5.08	4.7
$[Pd(\beta\text{-}ala)(tn)]^+$	2.48	2.68	5.16	3.9
$[Pd(N\text{-}Megly)(en)]^+$	2.78	2.73	5.51	−0.9
$[Pd(CH_3CO_2)_2(en)]$d)	2.63	3.01	5.65	6.7
$[Pd(CH_3CO_2)_2(tn)]$d)	3.05	2.80	5.85	−4.3
$[Pd(ox)(rac\text{-}pn)]$	2.58	2.74	5.32	3.0
$[Pd(ox)(tn)]$	2.31	2.54	4.85	4.7
$[Pd(mal)(rac\text{-}pn)]$	2.86	2.82	5.68	−0.7
$[Pd(mal)(tn)]$	2.64	2.70	5.35	1.1
$[Pd_2(\mu\text{-}OH)_2(en)_2]^{2+}$	3.06	2.73	5.79	−5.7
$[Pd_2(\mu\text{-}OH)_2(tn)_2]^{2+}$	2.70	2.67	5.37	−0.6
$[Pd(OH_2)_2(en)]^{2+}$e)	2.51	3.05	5.56	9.7
$[Pd(OH_2)_2(tn)]^{2+}$e)	2.61	3.07	5.68	8.1
$[Pd(OH)_2(tn)]$f)	2.68	2.78	5.47	1.8
$[Pd(CH_3CO_2)_2(gly)]^-$d)	2.41	2.99	5.40	10.7
$[Pd(mal)(gly)]^-$	2.95	3.05	6.00	1.7
$[Pd(ox)(\beta\text{-}ala)]^-$	2.38	2.40	4.79	0.4
$[Pd(mal)(\beta\text{-}ala)]^-$	2.53	2.78	5.32	4.7
$[Pd(ox)_2]^{2-}$	3.09	3.12	6.21	0.5
$[Pd(mal)_2]^{2-}$	2.75	2.76	5.52	0.2

a) $\varepsilon=\varepsilon_{max}/2$ at $\sigma=\sigma_{max}-\Delta\sigma^-$ and $\sigma_{max}+\Delta\sigma^+$; $\Delta\sigma_{1/2}=\Delta\sigma^-+\Delta\sigma^+$. b) unsymmetry parameter= $\{(\Delta\sigma^+-\Delta\sigma^-)/\Delta\sigma_{1/2}\}\times 100$. c) In acetonitrile. d) In 0.50 M CH_3CO_2Na. e) $[Pd_2(\mu\text{-}OH)_2(en\ or\ tn)_2](ClO_4)_2$ in 0.01 M $HClO_4$. f) $[Pd_2(\mu\text{-}OH)_2(tn)_2](ClO_4)_2$ in 0.01 M NaOH.

The substitution of β-ala for tn largely affect neither the band area nor the band width, but that of mal for β-ala does. An analogous behavior is also found in the series of en(or pn)-gly(or *S*-ala)-ox complexes except a pair of $[Pd(ox)(pn)]$ and $[Pd(gly)(en)]$ (Fig. 10).

The complexes containing tn, β-ala, or CH_3CO_2 generally possess oscillator strengths higher than the corresponding en(or pn), gly, or mal(or ox) complexes, respectively (Fig. 10). The exceptions are limited to the complexes with one tn and two unidentate ligands: $[Pd(CH_3CO_2)_2(tn)]$, $[Pd(OH)_2(tn)]$, and $[PdCl_2(tn)]$.[16] These complexes are expected to be less distorted than the corresponding en or *S*-pn complexes mainly in terms of bond angle. In other complexes, ligand-ligand interactions are presumed to be predominant. The complex $K_2[Pd(ox)_2]$ has the lowest oscillator strength among the palladium(II) complexes which we have so far investigated [$(\Delta\sigma_{1/2}\times\varepsilon)/10^5$ mol^{-1} dm^3 cm^{-2}=6.57; *cf.* $K_2[PdCl_4]$ (6.66)]. This may be attributable to the high planarity of the complex ion.

Figure 11 displays the unsymmetrical shape of the spin-allowed d-d absorption band. The complexes which exhibit an absorption band with a swelling in the higher or lower energy side are located on the lower right or upper left of the line $\Delta\sigma^+=\Delta\sigma^-$ (See the footnote of Table 9), respectively; the farther the complexes are located away from the line, the more unsymmetrical their band shapes are. The introduction of *N,N*-Et_2en(or N^1,N^1-Et_2-(*S*)-pn) in place of en(or *S*-pn) increases the band width mainly through the increase in $\Delta\sigma^-$. This behavior can be explained by supposing an increased transition energy difference between $^1A_{2g}$ and $^1E_g\leftarrow{}^1A_{1g}$ and/or the enhanced oscillator strength of $^1A_{2g}\leftarrow{}^1A_{1g}$. The location of the di-μ-hydroxo complex of en or S-pn in Fig. 11 may be also attributable to the relative lowering of the transition energy of $^1A_{2g}\leftarrow{}^1A_{1g}$.

The en or pn complexes of μ-OH, OH, mal, and ox are correlated with the corresponding tn complexes in a similar fashion (Fig. 11): the substitution of tn for en or pn decreases the band width with the decrease of $\Delta\sigma^-$ which is more substantial than that of $\Delta\sigma^+$.

The band shapes of the diaqua complexes are similar to each other irrespective of the kind of diamine ligands, whereas the diacetato complex with tn exhibits a band shape largely different from that of the corresponding complex with en or pn; thus, aqua and the diamine ligands have a predominant influence on the band shape in the former and the latter case, respectively. Similarly, tn and β-ala ligands seem to have a overwhelming influence on the band shape

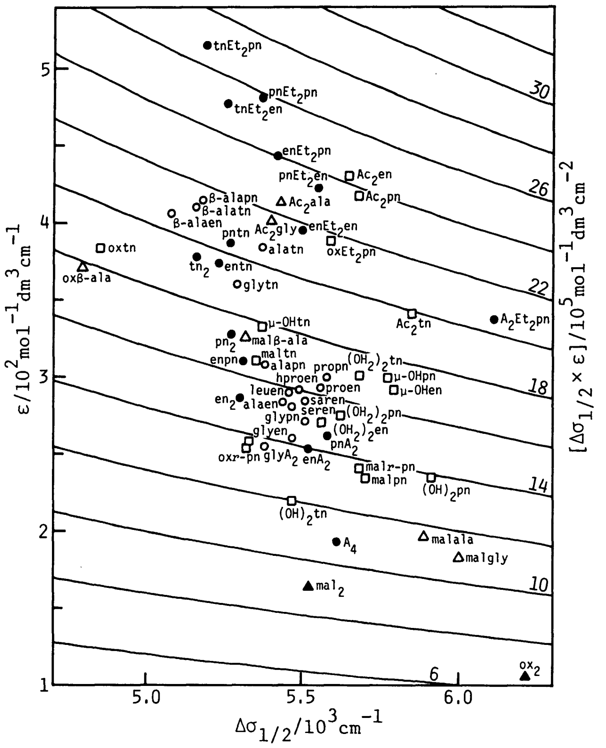

Fig. 10. Area intensity of the spin-allowed d-d absorption band represented as a function of the molar absorption coefficient of the absorption peak and the half-value width $\Delta\sigma_{1/2}$; ●: $[Pd(N)_4]$-, ○: $[Pd(N)_3(O)]$-, □: *cis*-$[Pd(N)_2(O)_2]$-, △: $[Pd(N)(O)_3]$-, and ▲: $[Pd(O)_4]$-type complexes; A=NH_3, pn=*S*-pn, *r*-pn=*rac*-pn, Et_2en=*N*,*N*-Et_2en, Et_2pn=N^1,N^1-Et_2-(*S*)-pn, ala=(*S*)-alaninato, ser=(*S*)-serinato, leu=(*S*)-leucinato, pro=(*S*)-prolinato, hpro=(*S*)-hydroxyprolinato, sar=sarcosinato, and Ac=acetato.

in the $[Pd(N)_4]$- and $[Pd(N)_3(O)]$-type complexes, respectively.

The complexes containing tn, *β*-ala, or ox possess a band width narrower than the corresponding en(or pn), gly, or mal complexes, respectively, except $[Pd(OH_2)_2(tn)]^{2+}$, $[Pd(CH_3CO_2)_2(tn)]$, $[Pd(\beta\text{-ala})(tn)]^+$, and $[Pd(ox)_2]^{2-}$.

The relationship between the absorption band width $\Delta\sigma_{1/2}$ and the MCD intensity ratio $|\Delta\varepsilon_M(+)/\Delta\varepsilon_M(-)|$ is visualized in Fig. 12; which includes the data for $[Pd(Cl)_n(N)_{4-n}]$(n=1,2, and 4) and *cis*-$[Pd(Cl)_2(N)(O)]$-type complexes in addition to those for the $[Pd(N)_n(O)_{4-n}]$-type ones and reveals two facts. Firstly, the complexes with tn have a larger value of $|\Delta\varepsilon_M(+)/\Delta\varepsilon_M(-)|$ than the corresponding en or pn complexes without exception. Secondly, the complexes which possess a smaller $\Delta\sigma_{1/2}$ value exhibit a larger $|\Delta\varepsilon_M(+)/\Delta\varepsilon_M(-)|$ value and *vice versa*. This relationship implies a possibility of the mixing between d-d vibronic excited states by applied magnetic field; and such a mixing is presumed to give a negative B term for the ${}^1A_{2g}\leftarrow{}^1A_{1g}$ transition depending upon the magnitude of the mixing, which should be inversely proportional to the energy gap involved.[17] Thus, the MCD features predominated by B terms can be qualitatively explained by the mixing of this kind and by the mixing between a d-d vibronic excited state and a CT excited state as proposed in the previous section.

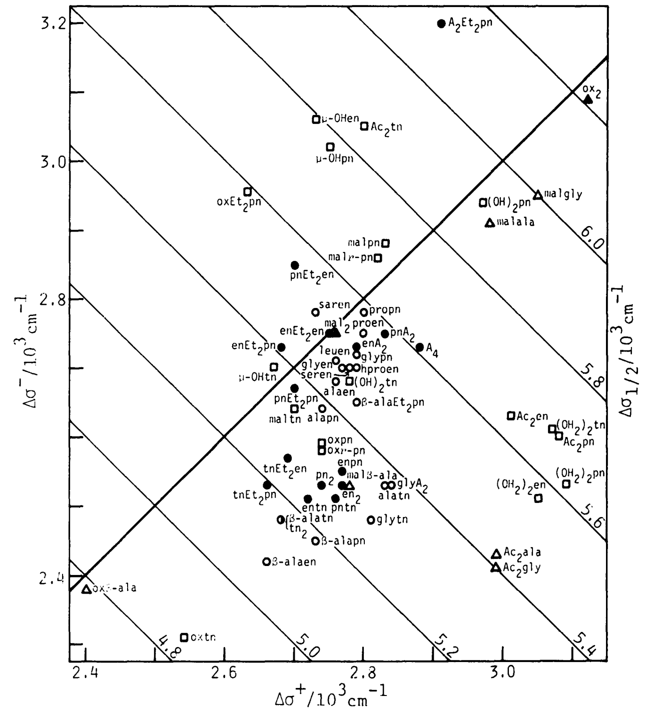

Fig. 11. Half-value width $\Delta\sigma_{1/2}$ (thin lines) represented as a function of $\Delta\sigma^+$ and $\Delta\sigma^-$; the thick line denotes $\Delta\sigma^+=\Delta\sigma^-$. See the footnote of Table 9 and the figure caption of Fig. 10 as to the marks and abbreviations.

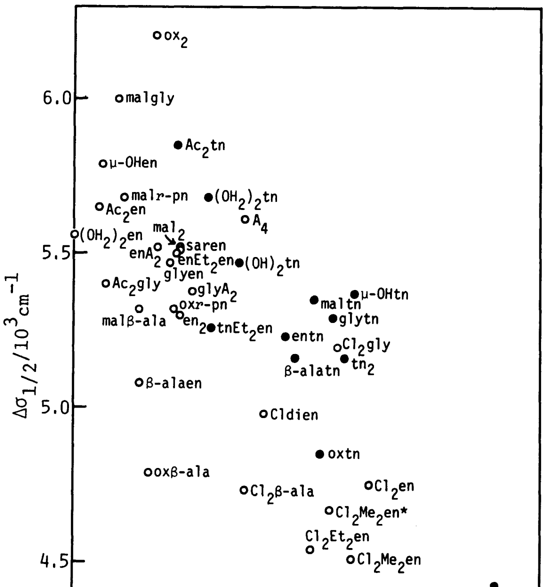

Fig. 12. Relationship between the half-value width $\Delta\sigma_{1/2}$ and the intensity ratio $|\Delta\varepsilon_M(+)/\Delta\varepsilon_M(-)|$; ●: complexes containing tn and ○: complexes not containing tn; Me_2en=*N*,*N*-Me_2en, Me_2en^*=*N*,*N'*-Me_2en, Me_2tn=*N*,*N*-Me_2tn, and dien=diethylenetriamine, and see the figure caption of Fig. 10 as to the other abbreviations.

References

1) K. Nakayama, T. Komorita, and Y. Shimura, *Bull. Chem. Soc. Jpn.*, **57**, 1336 (1984).

2) K. Nakayama, T. Komorita, and Y. Shimura, *Bull. Chem. Soc. Jpn.*, **57**, 1240 (1984).

3) K. Nakayama, T. Komorita, and Y. Shimura, *Bull. Chem. Soc. Jpn.*, **57**, 972 (1984).

4) K. Nakayama, T. Komorita, and Y. Shimura, *Bull. Chem. Soc Jpn.*, **54**, 1056 (1981). *N,N,C,C*-Me$_4$en=*N*^{2},*N*^{2}-dimethyl-2-methyl-1,2-propanediamine: $NH_2CH_2C(CH_3)_2N(CH_3)_2$; the abbreviation is based on the name for a substituted ethylenediamine.

5) M. Suzuki and Y. Nishida, *Inorg. Chim. Acta*, **34**, 61 (1979).

6) H. D. K. Drew, F. W. Pinkard, G. H. Preston, and W. Wardlaw, *J. Chem. Soc.*, **1932**, 1895.

7) J. S. Coe and J. R. Lyons, *Inorg. Chem.*, **9**, 1775 (1970).

8) E. A. Sullivan, *Can. J. Chem.*, **57**, 62 (1979).

9) The half-value-width parameters given in 10^3cm^{-1}: See the footnote of Table 9.

10) Prolonged heating gave the dimer complex [(β-ala)Pd(μ-Cl)$_2$Pd(β-ala)]. Found: C, 15.72; H, 2.74; N, 5.96%. Calcd for $C_6H_{12}N_2O_4Cl_2Pd_2$: C, 15.67; H, 2.63; N, 6.09%. This complex is sparingly soluble in water.

11) M. Vèzes, *Bull. Soc. Chim. Fr.*, **21**, 172 (1899).

12) G. Landesen, *Z. Anorg. Chem.*, **154**, 432 (1926).

13) M. J. Schmelz, I. Nakagawa, S. Mizushima, and J. V. Quagliano, *J. Am. Chem. Soc.*, **81**, 287 (1959).

14) The complex [Pd(CH$_3$CO$_2$)$_2$(NH$_3$)$_2$] was excluded owing to its lability for isomerization.

15) S. B. Piepho, P. N. Schatz, and A. J. McCaffery, *J. Am. Chem. Soc.*, **91**, 5994 (1969).

16) $(\Delta\sigma_{1/2}\times\varepsilon)/10^5$ mol^{-1} dm^3 cm^{-2}=13.3, 17.2, and 17.5 for [PdCl$_2$(tn)], [PdCl$_2$(en)], and [PdCl$_2$(*S*-pn)], respectively.

17) P. N. Schatz and A. J. McCaffery, *Quart. Rev.*, **23**, 552 (1969).